

Influence of the crystallographic orientation of silicon on the formation of „primary“ cracks

© V.I. Vettegren^{1,2}, A.G. Kadomtsev¹, I.P. Shcherbakov¹, R.I. Mamalimov^{1,2}, G.A. Oganessian¹

¹ Ioffe Institute,
St. Petersburg, Russia

² Schmidt Institute of Physics of the Earth, Russian Academy of Sciences,
Moscow, Russia

E-mail: Victor.Vettegren@mail.ru

Received December 29, 2021

Revised December 29, 2021

Accepted January 3, 2022

When the silicon surface is destroyed, clusters of the smallest „primary“ cracks are formed. Their formation leads to the appearance of „fractoluminescence“ (FL) signals. The FL signals and spectra contained maxima, the number of which is equal to the number of „primary“ cracks in the cluster. An analysis of the FL signals and spectra showed that, upon failure of the (100) and (110) surfaces, clusters of four „primary“ cracks appeared, and (111) surfaces, of three „primary“ cracks. Their sizes were estimated by the growth rate and time. It turned out that they are multiples of the crystal lattice constant a : $\approx 3a$, $4a$, and $6a$. At the moment of formation, „primary“ cracks are in a nonequilibrium state and, over time, transform into defects that look like „troughs“ and „tops“. Their sizes are from 2 to 4 times smaller than the sizes of „primary“ cracks.

Keywords: silicon, fracture, „primary“ cracks, fractoluminescence, interference profilometry.

DOI: 10.21883/PSS.2022.05.53516.268

1. Introduction

It is known that destruction of crystals exposed to mechanical stresses starts with formations, accumulation and combination of cracks [1–4]. The most small of them — „primary“ or „nucleating fractures“ — form when dislocations break the barriers that hinder their movement on the sliding planes [5–7].

To detect and study the „primary“ cracks on the surface (100) of silicon crystals in [8–10], fractoluminescence (FL) with time resolution 2 ns, white-light interference profilometry and photoluminescence methods were used. The question was: how the silicon surface orientation influences the formation of „primary“ cracks? To answer this question, we studied FL signals and spectra that occur during destruction of surfaces (100), (110), (111), and their profiles and PL spectra after destruction.

2. Research target and methods

„Primary“ cracks induced by destruction of silicon crystal surfaces (100), (110) and (111). The sample was destructed by two methods. The first method— cutting with a diamond saw. The second method involved FL excitation by an impact on a steel anvil placed perpendicularly to the sample surface.

The induced light (FL) was focused using a quartz lens on a cathode surface of PEM 136 photomultiplier tube. The output signal was applied to „ACTACOM“ ADS-3112 analog-to-digital converter input. The output voltage was

wrote to the PC memory every 2 ns. FL spectrum was recorded by AvaSpec-ULSi2048L-USB2 OE fiber-optic spectrometer.

Sample surface profiles were obtained using Zygo New View 6000 white-light interference profilometer at the Unique Scientific Unit „Physics, Chemistry, and Mechanics of Crystals and Thin Films“ (Institute for Problems in Mechanical Engineering of the Russian Academy of Sciences, St. Petersburg).

3. Fractoluminescence signals during formation of „primary“ cracks

Stresses applied to the crystals induce dislocation movement on sliding planes [5]. At plane intersections, barriers are formed and hinder the dislocation movement. Ultrafine „nucleating“ cracks are formed when the barriers are broken [6,7]. FL is induced by confinement during cracking [8–10].

Silicon crystal has a face-centered cubic lattice and contains 4 systems of intersecting dislocation sliding planes [111]. Therefore, FL spectra and signals shall contain 4 peaks each, and they are observed in FL spectra and signals of surfaces (100) and (110). However, only three peaks were observed in FL spectra and signals of surface (111) (Fig. 1).

It is known that the voltage acting on the dislocations is proportional to $m = \cos \chi \cdot \cos \lambda$, where λ is the angle between the external force and sliding direction, and χ is the angle between the force and normal to the sliding plane

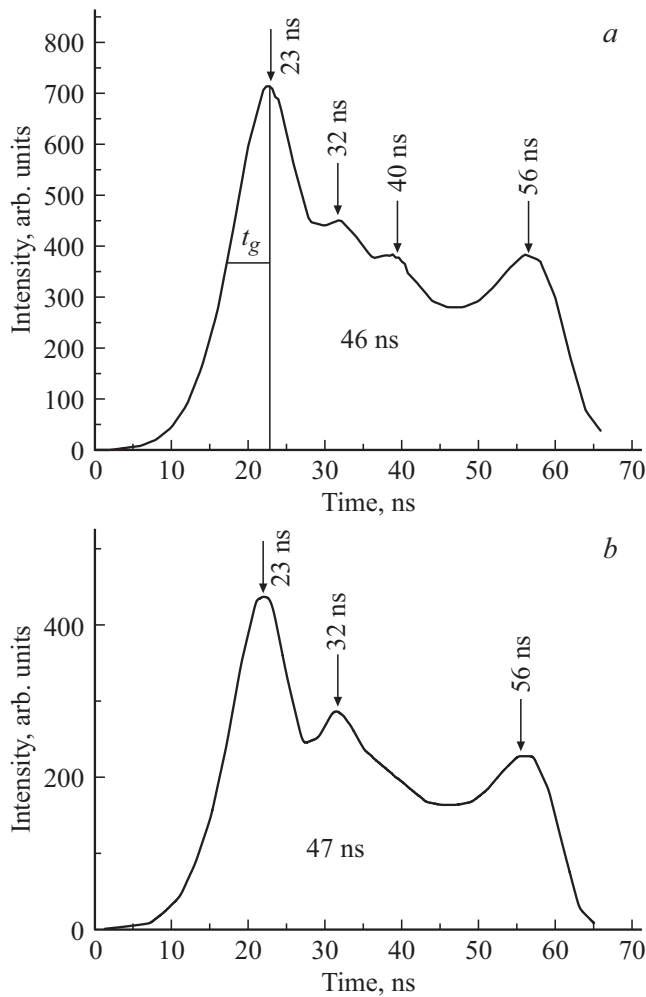


Figure 1. FL signals during destruction of surfaces (100) — (a) and (111) — (b).

(Schmid factor) [11]. The crack for which Schmid factor is the highest is the first to occur and grows faster than others. The first peak corresponds to it in FL signal (Fig. 1). For other planes, m is lower and leads to reduction of the „nucleating“ crack sizes. For direction (111), the third peak probably corresponds to the cracks for which $m \approx 0$.

The average signal existence time is ≈ 47 ns. The first peak appears ≈ 23 ns after the signal initiation, the second and third maxima for surfaces (100) and (110) appear at ≈ 9 ns intervals. And finally, the last FL signal for all surfaces is observed 33 ns after the first one.

The first peak is always the most intensive and, hence, the first crack is larger than the rest ones. The average intensity growing time of the first peak (at half-intensity) is $t_g \approx 8$ ns (Fig. 1). Assume that it is equal to the average velocity of anvil penetration into silicon. In our experiments, this velocity is ≈ 0.5 nm/ns. During 8 ns, the crack size l achieves ≈ 0.5 nm/ns \cdot 8 ns = 4 nm. The size of the second crack is ≈ 1.5 times lower than that of the first one and is equal to ≈ 2.6 nm. The size of the third (for lattice cell directions (100) and

Table 1. Primary crack edge lengths during destruction of silicon surfaces

| Orientation | Crack sizes, nm | | | |
|-------------|-----------------|---------|---------|---------|
| | (100) | 4(6)* | 2.6(4)* | 2.1(3)* |
| (110) | 4(6)* | 2.6(4)* | 2.0(3)* | 1.9(3)* |
| (111) | 4(6)* | 2.6(4)* | ? | 2.0(3)* |

Note. l/a values are given in brackets.

Table 2. Band peak energy in silicon FL spectra

| Surface | Energy, eV | | | |
|---------|------------|-----|-----|-----|
| | (100) | 1.4 | 1.6 | 1.8 |
| (110) | 1.4 | 1.7 | 1.9 | 1.9 |
| (111) | 1.41 | 1.6 | 1.7 | 2.1 |

(110)) and last cracks for all directions is ≈ 1.9 times lower than that of the first and is equal to ≈ 2 nm (Table 1).

Silicon crystal lattice constant (parameter) $a = 0.543$ nm [12]. If the ratio l vs. a is calculated,

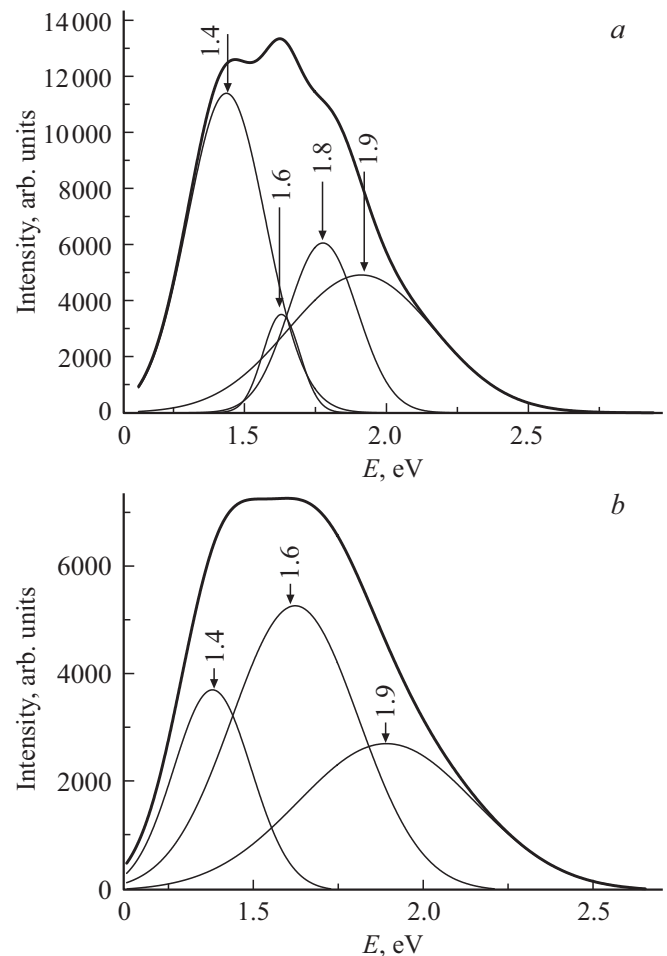


Figure 2. FL spectra of surfaces (100) — (a) and (111) — (b).

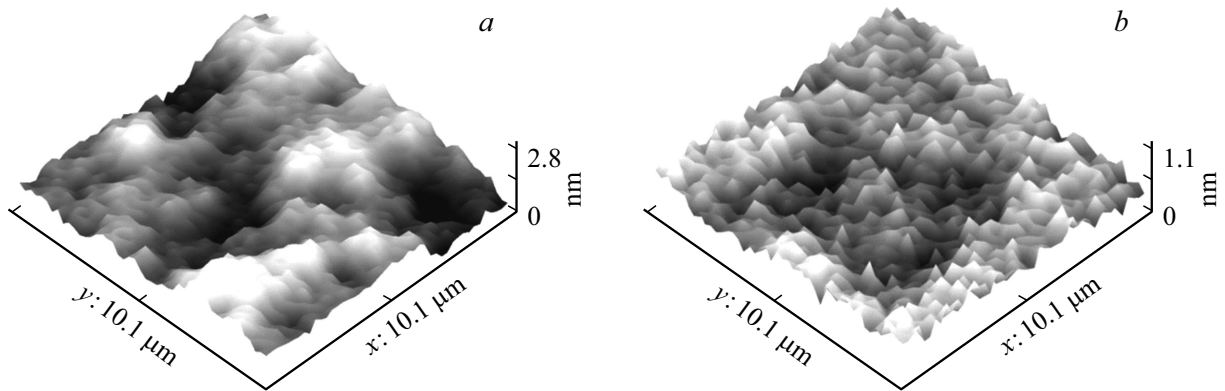


Figure 3. Surfaces (100) — (a) and (111) — (b).

it can be seen that the crack edge length changes approximately in multiples of the lattice constant and is equal to $\approx 3a, 4a$ and $6a$ (Table 1). Such small crack sizes prove that the cracks are correctly classified as „primary“.

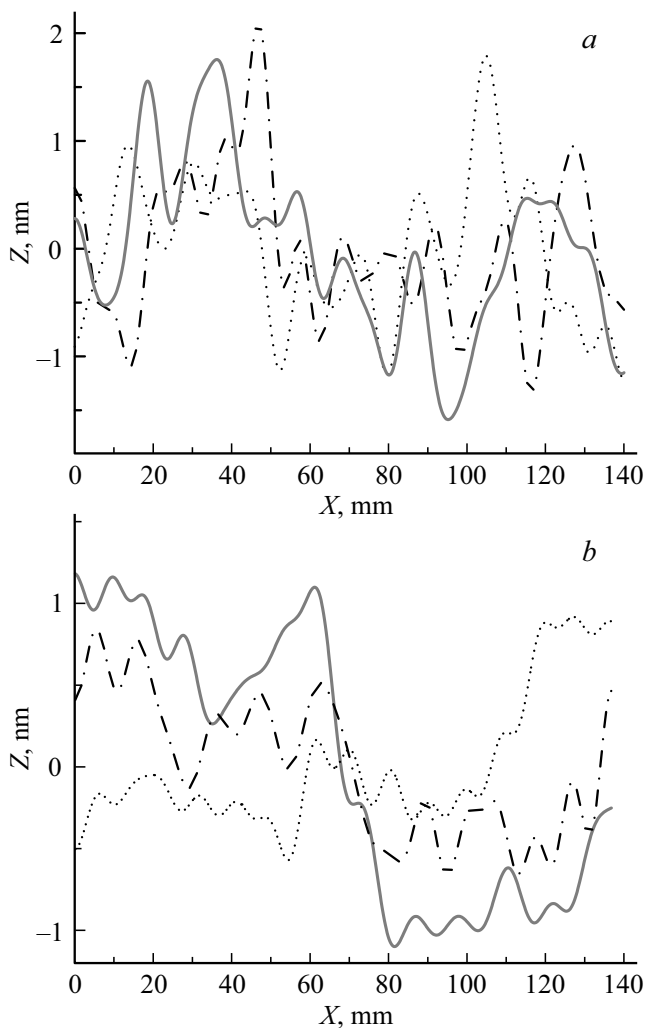


Figure 4. Surface cross-section profiles (100) — (a) and (111) — (b) parallel to axis X.

4. Fractoluminescence spectra during silicon destruction

Fig. 2 shows FL spectra that occur during initiation of „primary“ cracks. In FL spectra of surfaces (100) and (110), 4 bands are observed: 1.4, 1.6, 1.8 and 1.9 eV, and of surface (111) — 3 bands are observed: 1.4, 1.6 and 2 eV (Fig. 2, Table 2). It should be noted that band 1.8 eV is absent in FL spectra of surface (111). As mentioned above, peak at 39 ns is also absent in FL signals. This band may be probably assigned to cracks that form 39 ns after the cluster initiation. Assignment of the other bands in FL spectra is unclear.

5. Defects after crack relaxation on the silicon surfaces

„Primary“ cracks are in non-equilibrium state. Stresses near cracks relax with time and defects are formed in these areas. These defects were observed by the interference profilometry method. Fig. 3 shows surfaces (100) and (111) of the silicon samples after destruction. Both surfaces contain many defects: „tips“ and valleys. They were probably formed during relaxation of the „primary“ cracks.

To find the tip height distribution, surface cross-section profile parallel to axis X was made (Fig. 4). It was found that, on surfaces (100) and (110) it was a sum of four

Table 3. Structural nanodefekt height on surfaces (100) and (111)

| Surface | (100) | (110) | (111) |
|---------|------------|-----------|-----------|
| Tip No | Height, nm | | |
| 1 | 0.5(0.9)* | 0.5(0.9)* | 0.5(0.8)* |
| 2 | 1.0(1.4)* | 0.9(1.4)* | 1.1(1.7)* |
| 3 | 1.6(2.6)* | 1.7(2.6)* | 1.8(2.8)* |
| 4 | 2.4(3.5)* | 2.3(3.5)* | — |

Note. l/a . values are given in brackets.

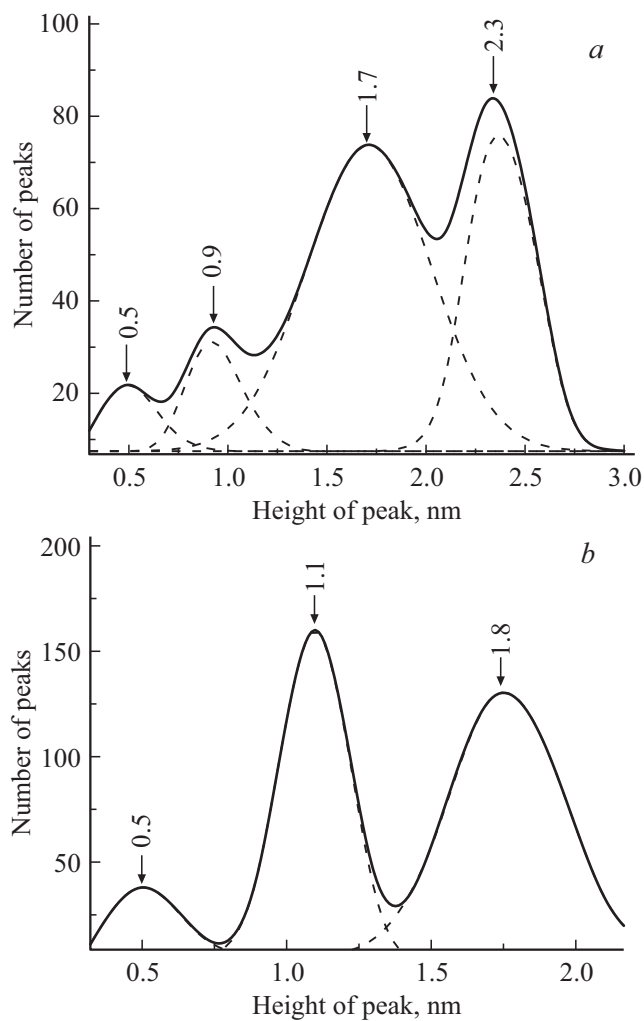


Figure 5. Structural feature height distribution on silicon surfaces (100) — (a) and (111) — (b).

Gaussian distributions of defects whose height h varied from ≈ 0.6 to ≈ 2.3 nm (Fig. 5, a, Table 3). At the same time, the height distribution of pyramids on surface (111) contained only 3 Gaussian distributions (Fig. 5, b). Their height varied from ≈ 0.5 to 1.8 nm (Table 3).

Fig. 5 and Table 3 show that the height of structural feature tips is $2\text{ to }4$ times lower than the sizes of „primary“ cracks.

6. Conclusion

1. During destruction of silicon surfaces (100), (110) and (111), „primary“ cracks are formed, the size l of which varies in multiples of the lattice constant a : $3a$; $4a$ and $6a$.

2. Stresses near the primary cracks relax with time and „pyramide“-like defects are formed in these areas. The size of these defects is $2\text{ to }4$ times smaller than the size of „primary“ cracks.

Conflict of interest

The authors declare that they have no conflict of interest.

References

- [1] P.G. Cheremsky, V.V. Slezov, V.I. Betekhtin. Pory v tviordom tele. Energoatomizdat, M. (1990). 376 p. (in Russian).
- [2] B.I. Betekhtin, A.G. Kadomtsev. FTT **47**, 5, 801 (2005) (in Russian).
- [3] V.R. Regel, A.I. Slutsker, E.E. Tomashevsky. Kineticheskaya priroda prochnosti tverdykh tel. Nauka, M. (1974). 560 p. (in Russian).
- [4] V.A. Petrov, A.Ya. Bashkarev, V.I. Vettegren'. Fizicheskie osnovy prognozirovaniya dolgovechnosti konstruktsionnykh materialov. Politekhnik, SPb (1993). 475 p. (in Russian).
- [5] A.N. Orlov. Vvedeniye v teoriyu defel'tov v kristallakh. Vyssh. shk., M. (1983). 144 p. (in Russian).
- [6] A.H. Cottrell. Theory of Crystal Dislocations. Gordon and Breach, N. Y. (1964). 91 p.
- [7] V.I. Vladimirov. Fizicheskaya priroda razrusheniya metallov. Metallurgiya, M. (1984). 280 p. (in Russian).
- [8] V.I. Vettegren', R.I. Mamalimov, I.P. Shcherbakov, V.B. Kulik. FTT **62**, 1070 (2020) (in Russian). DOI: 10.21883/FTT.2020.07.49475.041.
- [9] V.I. Vettegren, A.V. Ponomarev, R.I. Mamalimov, I.P. Scherbakov, V.B. Kulik. J. Phys.: Conf. Ser. **012142**, 1697 (2020). DOI: 10.1088/1742-6596/1697/1/012142.
- [10] V.I. Vettegren', A.G. Kadomtsev, I.P. Shcherbakov, R.I. Mamalimov, G.A. Oganesyana. FTT **63**, 1594 (2021) (in Russian). DOI: 10.21883/FTT.2021.10.51410.122.
- [11] E. Schmid, V. Boas. Kristallplastizität mit Besonderer Berücksichtigung der Metalle. Springer, Berlin (1935). 316 p.
- [12] O. Bisi, S. Ossicini, L. Pavesi. Surface Sci. Rep. **38**, 1 (2000).